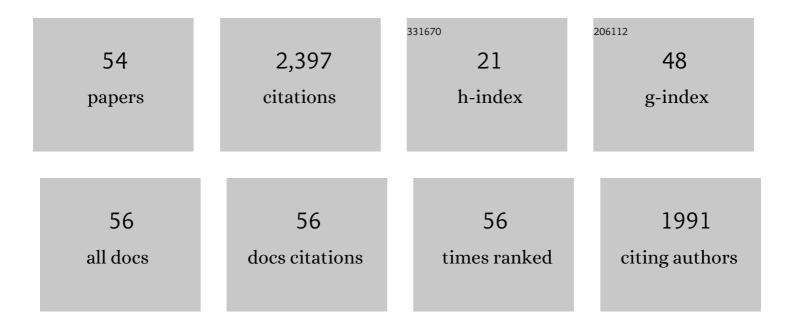
Stefano Benini

List of Publications by Year in descending order

Source: https://exaly.com/author-pdf/622063/publications.pdf Version: 2024-02-01



#	Article	IF	CITATIONS
1	A new proposal for urease mechanism based on the crystal structures of the native and inhibited enzyme from Bacillus pasteurii: why urea hydrolysis costs two nickels. Structure, 1999, 7, 205-216.	3.3	462
2	Chemistry of Ni ²⁺ in Urease: Sensing, Trafficking, and Catalysis. Accounts of Chemical Research, 2011, 44, 520-530.	15.6	224
3	The complex of Bacillus pasteurii urease with acetohydroxamate anion from X-ray data at 1.55 Ã resolution. Journal of Biological Inorganic Chemistry, 2000, 5, 110-118.	2.6	169
4	Structural properties of the nickel ions in urease: novel insights into the catalytic and inhibition mechanisms. Coordination Chemistry Reviews, 1999, 190-192, 331-355.	18.8	147
5	Molecular Details of Urease Inhibition by Boric Acid:Â Insights into the Catalytic Mechanism. Journal of the American Chemical Society, 2004, 126, 3714-3715.	13.7	142
6	Structure-based rationalization of urease inhibition by phosphate: novel insights into the enzyme mechanism. Journal of Biological Inorganic Chemistry, 2001, 6, 778-790.	2.6	132
7	The complex of Bacillus pasteurii urease with β-mercaptoethanol from X-ray data at 1.65-à resolution. Journal of Biological Inorganic Chemistry, 1998, 3, 268-273.	2.6	119
8	Urease from the soil bacterium Bacillus pasteurii: Immobilization on Ca-polygalacturonate. Soil Biology and Biochemistry, 1996, 28, 811-817.	8.8	92
9	The Structure of the Elusive Urease–Urea Complex Unveils the Mechanism of a Paradigmatic Nickelâ€Dependent Enzyme. Angewandte Chemie - International Edition, 2019, 58, 7415-7419.	13.8	66
10	Crystal Structure of OxidizedBacillus pasteuriiCytochromec553at 0.97-à Resolutionâ€. Biochemistry, 2000, 39, 13115-13126.	2.5	59
11	Fluoride inhibition of Sporosarcina pasteurii urease: structure and thermodynamics. Journal of Biological Inorganic Chemistry, 2014, 19, 1243-1261.	2.6	58
12	Structural basis for DNA recognition and loading into a viral packaging motor. Proceedings of the National Academy of Sciences of the United States of America, 2012, 109, 811-816.	7.1	57
13	The crystal structure of Erwinia amylovora levansucrase provides a snapshot of the products of sucrose hydrolysis trapped into the active site. Journal of Structural Biology, 2015, 191, 290-298.	2.8	56
14	Bacillus pasteurii urease: A heteropolymeric enzyme with a binuclear nickel active site. Soil Biology and Biochemistry, 1996, 28, 819-821.	8.8	55
15	The crystal structure of Sporosarcina pasteurii urease in a complex with citrate provides new hints for inhibitor design. Journal of Biological Inorganic Chemistry, 2013, 18, 391-399.	2.6	49
16	Biomolecular Characterization of the Levansucrase of Erwinia amylovora, a Promising Biocatalyst for the Synthesis of Fructooligosaccharides. Journal of Agricultural and Food Chemistry, 2013, 61, 12265-12273.	5.2	45
17	Kinetic and structural studies reveal a unique binding mode of sulfite to the nickel center in urease. Journal of Inorganic Biochemistry, 2016, 154, 42-49.	3.5	42
18	X-ray Absorption Spectroscopy Study of Native and Phenylphosphorodiamidate-Inhibited Bacillus pasteurii Urease. FEBS Journal, 1996, 239, 61-66.	0.2	31

STEFANO BENINI

#	Article	IF	CITATIONS
19	Modulation of Bacillus pasteurii cytochrome c 553 reduction potential by structural and solution parameters. Journal of Biological Inorganic Chemistry, 1998, 3, 371-382.	2.6	28
20	Holo-Ni2+Helicobacter pylori NikR contains four square-planar nickel-binding sites at physiological pH. Dalton Transactions, 2011, 40, 7831.	3.3	28
21	A complete structural characterization of the desferrioxamine E biosynthetic pathway from the fire blight pathogen Erwinia amylovora. Journal of Structural Biology, 2018, 202, 236-249.	2.8	26
22	Crystallization and preliminary high-resolution X-ray diffraction analysis of native and β-mercaptoethanol-inhibited urease from Bacillus pasteurii. Acta Crystallographica Section D: Biological Crystallography, 1998, 54, 409-412.	2.5	21
23	Enzymatic synthesis of nucleobase-modified UDP-sugars: scope and limitations. Carbohydrate Research, 2015, 404, 17-25.	2.3	21
24	The Impact of pH on Catalytically Critical Protein Conformational Changes: The Case of the Urease, a Nickel Enzyme. Chemistry - A European Journal, 2019, 25, 12145-12158.	3.3	21
25	Conservation of Erwinia amylovora pathogenicity-relevant genes among Erwinia genomes. Archives of Microbiology, 2017, 199, 1335-1344.	2.2	17
26	An Unusual, His-dependent Family I Pyrophosphatase from Mycobacterium tuberculosis. Journal of Biological Chemistry, 2005, 280, 41819-41826.	3.4	16
27	Cloning, expression, purification, crystallization and preliminary X-ray analysis of <i>Ea</i> Lsc, a levansucrase from <i>Erwinia amylovora</i> . Acta Crystallographica Section F: Structural Biology Communications, 2013, 69, 570-573.	0.7	15
28	The Structure of Sucrose-Soaked Levansucrase Crystals from Erwinia tasmaniensis reveals a Binding Pocket for Levanbiose. International Journal of Molecular Sciences, 2020, 21, 83.	4.1	15
29	Glucose-1-phosphate uridylyltransferase from Erwinia amylovora : Activity, structure and substrate specificity. Biochimica Et Biophysica Acta - Proteins and Proteomics, 2017, 1865, 1348-1357.	2.3	13
30	Comparison of the Levansucrase from the epiphyte Erwinia tasmaniensis vs its homologue from the phytopathogen Erwinia amylovora. International Journal of Biological Macromolecules, 2019, 127, 496-501.	7.5	13
31	Oxidized and Reduced [Fe2Q2] (Q = S, Se) Cores of Spinach Ferredoxin: a Comparative Study Using 1H NMR Spectroscopy. Inorganic Chemistry, 1995, 34, 417-420.	4.0	12
32	Structure ofRhodoferax fermentanshigh-potential iron–sulfur protein solved by MAD. Acta Crystallographica Section D: Biological Crystallography, 2003, 59, 1582-1588.	2.5	12
33	The structure of Erwinia amylovora AvrRpt2 provides insight into protein maturation and induced resistance to fire blight by Malus ×â€⁻robusta 5. Journal of Structural Biology, 2019, 206, 233-242.	2.8	12
34	Carbohydrate-Active Enzymes: Structure, Activity, and Reaction Products. International Journal of Molecular Sciences, 2020, 21, 2727.	4.1	12
35	Cytochrome c-553 from the Alkalophilic Bacterium Bacillus pasteurii Has the Primary Structure Characteristics of a Lipoprotein. Biochemical and Biophysical Research Communications, 1999, 264, 380-387.	2.1	11
36	Two-wavelength MAD phasing: in search of the optimal choice of wavelengths. Acta Crystallographica Section D: Biological Crystallography, 1999, 55, 1449-1458.	2.5	9

STEFANO BENINI

#	Article	IF	CITATIONS
37	Crystals of cytochrome c-553 fromBacillus pasteurii show diffraction to 0.97 å resolution. Proteins: Structure, Function and Bioinformatics, 1997, 28, 580-585.	2.6	8
38	High resolution crystal structure of Rubrivivax gelatinosus cytochrome c′. Journal of Inorganic Biochemistry, 2008, 102, 1322-1328.	3.5	8
39	Characterization and 1.57â€Ã resolution structure of the key fire blight phosphatase AmsI from <i>Erwinia amylovora</i> . Acta Crystallographica Section F, Structural Biology Communications, 2016, 72, 903-910.	0.8	8
40	A genome-wide analysis of desferrioxamine mediated iron uptake in Erwinia spp. reveals genes exclusive of the Rosaceae infecting strains. Scientific Reports, 2019, 9, 2818.	3.3	8
41	Structure of theMycobacterium tuberculosissoluble inorganic pyrophosphatase Rv3628 at pHÂ7.0. Acta Crystallographica Section F: Structural Biology Communications, 2011, 67, 866-870.	0.7	7
42	Expression, purification, crystallization and preliminary X-ray analysis of glucose-1-phosphate uridylyltransferase (GalU) from <i>Erwinia amylovora</i> . Acta Crystallographica Section F, Structural Biology Communications, 2014, 70, 1249-1251.	0.8	7
43	The Structure of the Elusive Urease–Urea Complex Unveils the Mechanism of a Paradigmatic Nickelâ€Dependent Enzyme. Angewandte Chemie, 2019, 131, 7493-7497.	2.0	7
44	The structural and functional characterization of Malus domestica double bond reductase MdDBR provides insights towards the identification of its substrates. International Journal of Biological Macromolecules, 2021, 171, 89-99.	7.5	6
45	Cyclic voltammetry and spectroelectrochemistry of cytochrome c8 from Rubrivivax gelatinosus. Implications in photosynthetic electron transfer. Inorganica Chimica Acta, 1997, 263, 379-384.	2.4	5
46	The 1.58â€Ã resolution structure of the DNA-binding domain of bacteriophage SF6 small terminase provides new hints on DNA binding. Acta Crystallographica Section F: Structural Biology Communications, 2013, 69, 376-381.	0.7	5
47	Cloning, purification, crystallization and 1.57â€Ã resolution X-ray data analysis of AmsI, the tyrosine phosphatase controlling amylovoran biosynthesis in the plant pathogenErwinia amylovora. Acta Crystallographica Section F, Structural Biology Communications, 2014, 70, 1693-1696.	0.8	4
48	Structural and functional analysis of Erwinia amylovora SrlD. The first crystal structure of a sorbitol-6-phosphate 2-dehydrogenase. Journal of Structural Biology, 2018, 203, 109-119.	2.8	4
49	The crystal structure of Erwinia amylovora AmyR, a member of the YbjN protein family, shows similarity to type III secretion chaperones but suggests different cellular functions. PLoS ONE, 2017, 12, e0176049.	2.5	3
50	Purification, crystallization and preliminary X-ray analysis of an acetylxylan esterase fromBacillus pumilus. Acta Crystallographica Section D: Biological Crystallography, 2001, 57, 1906-1907.	2.5	2
51	Structural and functional characterization of proteins from the fire blight pathogen Erwinia amylovora. A review on the state of the art. Journal of Plant Pathology, 2021, 103, 51-63.	1.2	2
52	Urease. , 2013, , 2287-2292.		1
53	Crystallization and preliminary X-ray diffraction analysis of cytochromec′ fromRubrivivax gelatinosusat 1.3â€Ã resolution. Acta Crystallographica Section D: Biological Crystallography, 1998, 54, 284-287.	2.5	0
54	The crystal structure of Rv2991 from Mycobacterium tuberculosis: An F420 binding protein with unknown function. Journal of Structural Biology, 2019, 206, 216-224.	2.8	0